Materials and Structures (2023) 56:168
https://doi.org/10.1617/s11527-023-02249-y

ORIGINAL ARTICLE

Chemical and mechanical analysis of VAPro-aged asphalt binders from different crude oil sources

Daniel Maschauer · Daniel Steiner · Johannes Mirwald · Bernhard Hofko

Received: 1 March 2023 / Accepted: 21 September 2023 / Published online: 19 October 2023

Abstract Asphalt binders change their properties over time under natural and anthropogenic influences since they are of organic origin. This leads to a deterioration of the mechanical behavior and, thus to higher stiffness and brittleness of the binder. This phenomenon is commonly known as "aging." As a consequence, these changes have a negative impact on the low temperature and fatigue behavior of asphalt mix layers. The standardized RTFOT for STA and PAV for LTA are used to simulate aging in the laboratory on the bitumen scale. On the asphalt mix scale, various methods have been developed for either loose material or compacted specimens. This paper presents a recently developed conditioning method called the "Viennese Aging Procedure" (VAPro) for long-term aging of compacted HMA specimens at close-to-field conditions (T = 60°C and $p \leq 1$ bar). Air enriched with traces of highly oxidizing gases (ozone and nitrogen oxides) is passed through the specimens to enhance the oxidation reaction. The chemical reactions triggered by VAPro are expected to be similar to field aging. The applicability of the method is demonstrated. Mixtures containing four binders of the same grade were aged. Significant differences in aging behavior can be observed. The VAPro-aging is about 1.2 to 2.6 times stronger than that of PAV in terms of stiffness increase on the binder level. The mechanical analysis is extended with FTIR measurements. It is shown that this method is of great use in evaluating aging behavior and detecting poorly performing binders.

Keywords VAPro · Long-term aging · Ozone · Nitrogen oxides · DSR · FTIR

1 Introduction

Asphalt mixtures are a widely used material in the road pavement industry. For example, Europe produced 280 million tons of hot and warm mix asphalt in 2019. This composite material uses bitumen obtained by crude oil refinement as a binder [1].

Due to the oxidation of bitumen as an organic material, the visco-elastic properties change over time. This leads to increased stiffness and brittleness, which results in the deterioration of the performance of the respective asphalt mixtures. The aging of asphalt binders and mixtures is divided into short-term aging (STA) and long-term aging (LTA). STA occurs during production and paving and is characterized by fast oxidation and vaporization of remaining volatile components due to high temperatures. LTA is a

D. Maschauer (✉) · D. Steiner · J. Mirwald · B. Hofko
Christian Doppler Laboratory for Chemo-Mechanical Analysis of Bituminous Materials, Institute of Transportation, TU Wien, Gusshausstrasse 28/E230-3, 1040 Vienna, Austria
e-mail: daniel.maschauer@tuwien.ac.at

slower process occurring during the service life of asphalt pavements. Natural and anthropogenic impacts trigger slow oxidation, particularly in the upper centimeters of (dense) asphalt pavements. The main impact factors are reactive oxygen species (ROS) in the atmosphere, like ozone (O_3) or nitrogen oxides (NO_x), UV/solar radiation, and moisture [2–9].

Accelerated aging simulation of bituminous materials is a time-efficient tool to predict long-term changes in material behavior. This information can be used for mix design optimization and thus, help to extend the asphalt pavements' lifetime and increase their recyclability by selecting the most suitable binder and ultimately developing more durable mixtures. Two methods are commonly used on the bitumen scale: For STA, the Rolling Thin Film Oven Test (RTFOT) is a reliable procedure to simulate production and mixing. For LTA, Pressure Aging Vessel (PAV) imitates a service life of 5 to 10 years [10, 11]. Various procedures have been developed on asphalt mix scale: They differ by either conditioning compacted specimens or loose mix and aging medium. Many methods use high temperatures (above + 100 °C) and/or high pressures that do not occur in the field [12, 13] to achieve long-term aging in a time-efficient manner. Due to these temperature and/or pressure differences, other reaction mechanics and kinetics can participate in the oxidation mechanism and thus differ from field aging.

A new procedure for aging compacted cylindrical asphalt mix specimens has been developed recently. The so-called "Viennese Aging Procedure" (VAPro) uses a highly reactive gas mixture to age the asphalt specimens in conditions similar to the field (+ 60 °C and pressure < 0.5 bar) [14, 15]. The gas mixture contains traces of reactive oxygen species (ROS), which are ozone (O_3) and nitrogen oxides (NO_x). These oxidants are also present in the atmosphere but in lower concentrations. Besides OH-radicals, O_3 and NO_x play a significant role in the tropospheric cycle. Thus, being one of the main drivers of tropospheric aging processes, they contribute to the idea of a realistic aging simulation [16–19]. Prior studies have shown the significant contribution of O_3 and NO_x on asphalt aging [20].

The aging of compacted specimens is reported to produce an aging gradient within the specimen when using oven aging or UV aging. This reflects the aging gradient occurring in the field [21, 22]. However, homogeneous oxidation is more suitable for material testing and assessment. Having this in mind, the idea of VAPro is as follows: By perfusing compacted specimens (1.0 l/min) with the above-mentioned reactive gas mixture, more homogeneous aging is targeted. Consequently, an air void content of at least 6.0% by volume is needed to maintain a sufficient gas flow through the specimens.

The main objective of this paper is to evaluate the applicability of VAPro. Therefore, asphalt mixes with the same grading curve but with bitumen of different origins are produced and aged with VAPro. At the same time, the binders are aged with RTFOT and PAV. For binder evaluation, the binders of the VAPro-aged specimens are extracted with tetrachloroethylene as a solvent and distilled according to EN 12697–3 [23]. The binders are analyzed by Dynamic Shear Rheometer (DSR) and Fourier-Transform Infrared (FTIR) Spectroscopy.

2 Materials and methods

2.1 Materials

This study uses asphalt concrete following EN 13108–1 [24] with a maximum nominal grain size of 11 mm (AC11) and a binder content of 5.2% by mass. Figure 1 shows the grading and limiting curves according to EN 13108–1. The fine and coarse

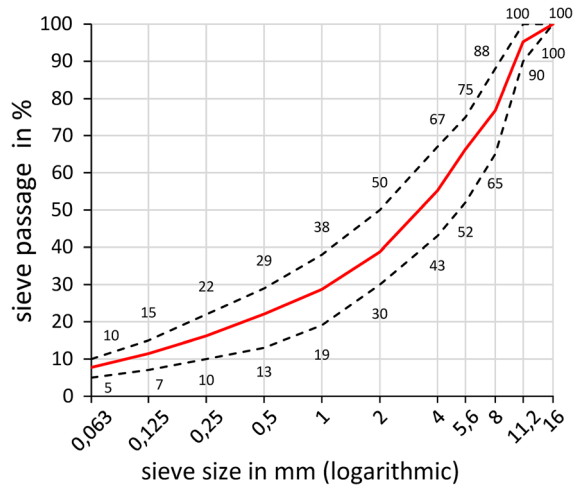

Fig. 1 Sieving curve of the used asphalt mixture

Table 1 Binder characteristics

Binder	Penetration in 1/10mm	Softening point in °C	PG-grade	Color code
1	85	45.4	64–28	Green
2	77	46.2	70–22	Orange
3	77	47.1	64–22	Red
4	79	47.2	64–22	Black

aggregates of the mix are of porphyritic origin, and the filler material is powdered limestone.

Four asphalt binders of the same grade (70/100 pen according to EN 12591 [25]) were selected from different sources to produce four mixes differing only in the binder used. In Table 1, various binder specifications are given for comparison. Since they are all graded the same, all four binders have similar values within the allowed limits. According to EN 12697–35 [26], a laboratory mixer is used to prepare the mixture at a temperature of + 170 °C. HMA slabs (50 × 26 × 4 cm) are compacted using a steel roller segment compactor according to EN 12697–33 [27].

From each slab, eight specimens with a diameter of 100 mm are cored. According to EN 12697–8 [28], the air void content of the specimens ranges from 4.8 to 9.2% by volume. The bulk density required for the void content calculation is determined according to EN 12697–6, procedure B [29]. For each mix, three specimens with an air void content of 7.0% ± 1.0% by volume are selected for aging. This relatively high air void content is necessary for VAPro-aging. The reasons for this are described in detail below.

2.2 Methods

2.2.1 Aging procedures

Rolling thin film oven test (RTFOT) and pressure aging vessel (PAV). All four virgin binders are aged in RTFOT according to EN 12607–1 [30] at + 163 °C. Subsequently, PAV is carried out according to EN 14769 [31] at + 100 °C and 2.1 MPa.

The Viennese aging procedure (VAPro). In the meantime, two independent aging cells have been developed: VAPro^{cyl} for aging up to three cylindrical specimens with a diameter of 100 mm and VApro^{pri} to obtain prismatic specimens [14, 32]. The asphalt mix specimens in this study are aged with VAPro^{cyl}. A single specimen is conditioned during each aging cycle. The centerpiece of this method is an ozone generator that produces a gas mixture containing traces of ROS. The gas mixture is produced by directing air from the central laboratory supply through the ozone generator. Using a dielectric discharge tube, the generator enriches the air with ozone and nitrogen oxides. The aging cell of VAPro^{cyl} is a triaxial cell in which the specimen is located and covered with a silicone membrane. Figure 2a shows the aging cell. An overpressure of ∼ 1.0 bar in the triaxial cell ensures that the elastic membrane is pressed against the specimen to maintain the gas flow through the specimen. A flow meter and a pressure regulator upstream of the generator ensure a constant flow (∼ 1.0 l/min) and pressure ($p \leq 1$ bar) in the system. A heating device is installed between the generator and the triaxial cell to heat the gas. The triaxial cell and the heating device are placed in a heating cabinet at a temperature of + 60 °C (= T_{oven}). In Fig. 2b, schematics of the VAPro principle are shown.

The aging duration was reduced compared to earlier studies since VAPro was continuously improved [15, 33]. With the latest setup, the aging duration was set to three days since the extracted binders achieved at least a level of RTFOT + PAV-aging after this duration [20]. After passing the triaxial cell, the gas mixture is led through a washing flask filled to degrade the ROS before the gas is sucked away by a fume hood.

2.2.2 Mechanical analysis

Binder extraction and recovery. To analyze the binders from the asphalt mixes, they are extracted with tetrachloroethylene as a solvent and distilled according to EN 12697–3 [23].

Binder testing. A DSR, according to EN 14770 [34], is used to investigate the rheology of the binders. A 25 mm plate with a gap of 1 mm is used in the upper-temperature range from + 40 °C to + 82 °C; from −4 °C to + 40 °C, an 8 mm plate with a gap of

Fig. 2 **a** photo of the aging cell (with cut-out to see the specimen), **b** VAPro schematics

2 mm is used. A strain-controlled frequency sweep is carried out from 0.1 Hz to 40 Hz. Dynamic Shear Modulus |G*| and phase angle δ are obtained from these measurements.

Mastercurve construction. Based on the time–temperature superposition principle (TTSP), the relationship between frequencies and temperatures allows us to gain information on material behavior on a broader scale than what is measurable. The modified Williams–Landel–Ferry (WLF) function proposed by Kaelble [35] is used to determine the time–temperature shift factors. Rowe and Sharrock [36] rearranged the original function for easier application, as shown in Eq. (1).

$$\log a_T = -C_1\left(\frac{T - T_k}{C_2 + |T - T_k|} - \frac{T_{ref} - T_k}{C_2 + |T_{ref} - T_k|}\right) \tag{1}$$

The mastercurves of |G*| and δ are determined using the Generalized Logistic Sigmoidal Model [37, 38]. Originally proposed for asphalt mixtures, Yusoff, et al. [39] demonstrated that the Generalized Logistic Sigmoidal Model shows a better correlation between measured and fitted data than CA or CAM models. The function used to calculate |G*| and δ mastercurves are shown in Eqs. (2) and (3).

$$|G^*| = \partial + \frac{\alpha}{\left[1 + \lambda e^{\beta+\gamma(\log(fr))}\right]^{1/\lambda}} \tag{2}$$

$$\delta = \frac{90\alpha\gamma e^{\beta+\gamma(\log(fr))}}{\left[1 + \lambda e^{\beta+\gamma(\log(fr))}\right]^{(1+1/\lambda)}} \tag{3}$$

The mastercurves are constructed with a widely known calculation software using non-linear least squares regression techniques. The best fit is found by minimizing the sum of squared errors (SSE) between measured and fitted data. From the mastercurve calculations, a variety of parameters can be obtained:

- Crossover Temperature T_c
- Crossover frequency f_c
- Crossover Modulus G_c
- The rheological parameter R
- G-R parameter

The crossover temperature T_c (where the phase angle is 45°) increases with aging. As aging progresses, the elastic behavior becomes more dominant at the given frequency. Thus, a higher reference temperature must be applied to reach the desired transition point. This parameter is successfully used in literature to describe the aging of asphalt binders [40–43].

At the same time, the crossover frequency f_c becomes lower with aging. The crossover modulus G_c (at f_c where G' = G'') undergoes the same evolution. The rheological parameter R (R-value) is an interesting parameter for mastercurve assessment. It describes the relation between G_c and the glassy modulus G_g ($G_g = 10^9$ MPa) and is expressed by the log of the ratio of G_g and G_c. The R-value increases with aging. Thus, lower values mean more favorable

mechanical performance. It was identified in the SHRP program as sensitive to aging and is widely used to evaluate bituminous binders [44–46].

For evaluation of susceptibility to embrittlement and cracking, the G-R parameter introduced by Glover, et al. [47] and rearranged by Rowe, et al. [48] (see Eq. 4) is used. The G-R parameter is calculated at 15 °C and 0.005 rad/s. For this study, the input for the G-R parameter is obtained from constructed mastercurves at 15 °C.

$$G - R = \frac{G^* * (\cos \delta)^2}{\sin \delta} \quad (4)$$

Rowe, et al. [48] suggests a warning limit for damage onset at 180 kPa and a critical limit for significant cracking at 600 kPa. Thus, a higher G-R parameter indicates increased embrittlement.

Four mastercurves for each sample are constructed at T_c, 15, 25 and 35 °C. This allows for a small statistical analysis of the master curve design: The temperature-independent parameters R and crossover modulus show a very small standard deviation of a maximum of 0.1%.

The Crossover temperature is obtained by running through the calculation procedure with the reference temperature as a variable. The frequency turns into the reference value and is set to 1.59 Hz. In addition, the requirement is set that at the given frequency phase angle has to be at 45°. Thus, the reference frequency becomes the crossover frequency at the same time here. The calculated crossover temperature (and the mastercurve construction) is validated by comparing it with the crossover temperature retrieved from the 8 mm plate DSR measurements by linear interpolation. Figure 3 shows an excellent correlation between the measured and calculated crossover temperature. The model slightly underestimates the crossover temperature.

2.2.3 *Chemical analysis*

Fourier-transform infrared (FTIR) spectroscopy. A Bruker Alpha II with an ATR diamond crystal module is used for the FTIR measurements. For each binder sample, four individual samples are measured. A background scan of the empty crystal is recorded before every measurement. For each sample, the device performs four consecutive measurements

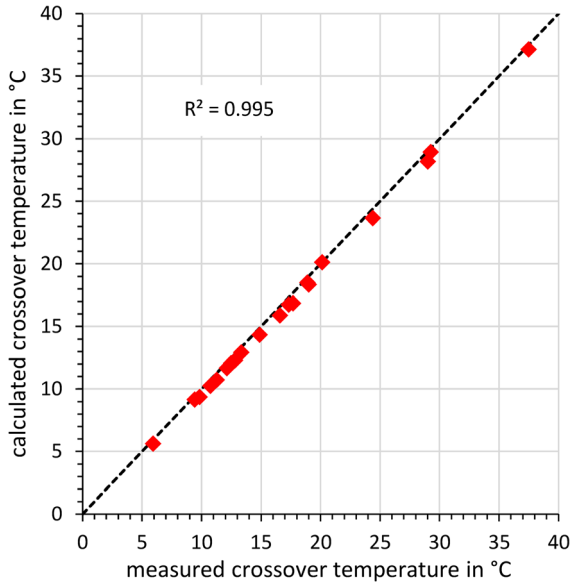

Fig. 3 Correlation between measured and calculated crossover temperature

considering 24 scans. This results in 16 single measurements per binder sample. The spectra are recorded within the wavelength range of 600—4000 cm^{-1} at a resolution of 4 cm^{-1}.

Sample preparation is as follows: A small amount of binder is heated to 130–160 °C on a spoon and homogenized. Heating and homogenizing are done within 60–120 s. The temperature is measured with a thermometer which is used for stirring at the same time. Next, four droplets per sample are applied on small pieces of silicone foil, which are then covered with a tin lid. The droplets cool down for 5 to 10 min before being applied to the ATR crystal for measurement.

The measured spectra are normalized in the fingerprint area from 600–1900 cm^{-1} using min/max normalization. The minimum can be found in the wavelength range of 1900–1800 cm^{-1}, where no functional group appears. The maximum is located around 1460 cm^{-1}, where the aliphatic band for reference appears. This approach results in less scattering due to the noise/artifacts generated by the ATR crystal in the wavelength range of 1950–2250 cm^{-1}. Figure 4 shows two example spectra of a virgin and an LTA-aged binder: The increase in carbonyl and sulfoxide bands with aging is easily identified. The box illustrates the random noise found in the lowest part of the spectra that can bias the analysis.

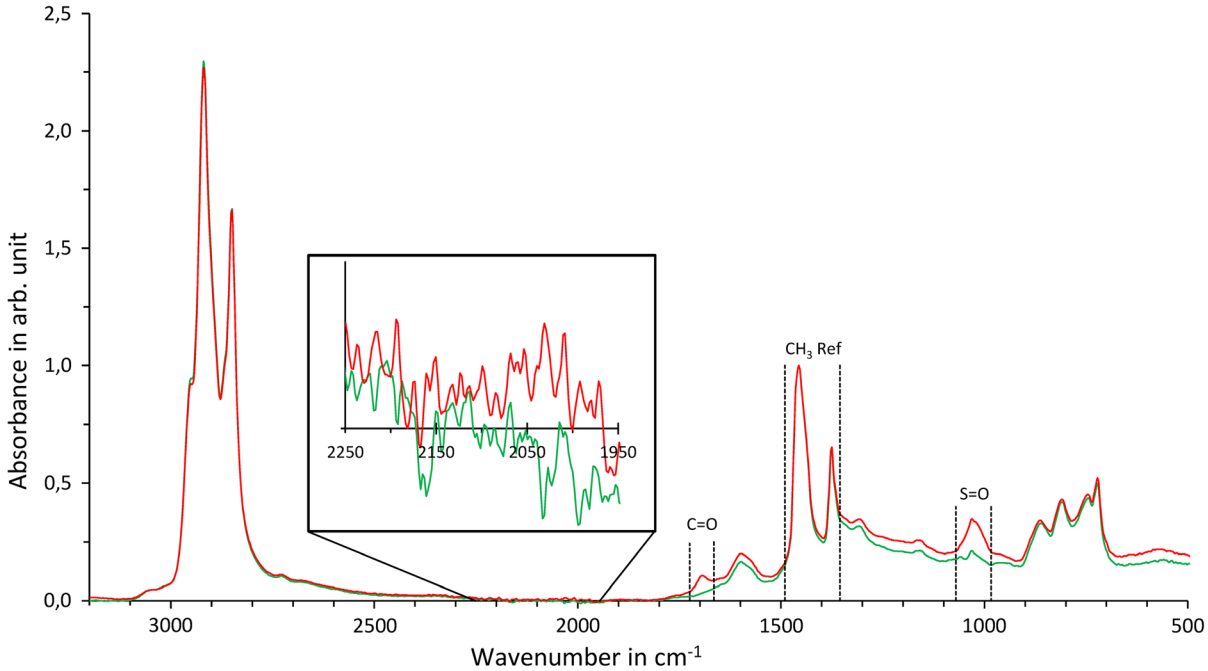

Fig. 4 Normalized FTIR spectra examples of an unaged and LTA-aged binder, including the illustration of the signal noise part around 1950–2250 cm^{-1}

For binder assessment, the following integrations are made by using the full baseline integration method:

- Carbonyls (AI_{CO}): wavelength band: 1665–1725 cm^{-1}
- Sulfoxides (AI_{SO}): wavelength band: 984–1070 cm^{-1}
- Reference aliphatic band (AI_{CH3}): wavelength band: 1355–1490 cm^{-1}

The Carbonyl Index $I_{C=O}$ and Sulfoxide Index $I_{S=O}$ are calculated by formulas (5) and (6) from these integrals. The Sulfoxide Index $I_{S=O}$ is not adopted for further analysis: Inconsistencies can be found in $I_{S=O}$ data when using recovered binders from asphalt mixtures. Some interactions with the aggregates during mixing or minimal amounts of left filler in the bitumen samples might bias the measurements, leading to dubious results [46, 49]. Similar effects are found within the analyzed data for this paper. Therefore, this work uses only the carbonyl index for chemical analysis. More research on this specific issue is needed.

$$I_{CO} = \frac{AI_{CO}}{AI_{CH_3}} \tag{5}$$

$$I_{SO} = \frac{AI_{SO}}{AI_{CH_3}} \tag{6}$$

3 Results and discussion

As described in part 2.2, all four binders in their five aging states (Virgin, RTFOT, RTFOT + PAV, LAB - MIX (= after slab production), VAPro) are analyzed by DSR and FTIR.

Figure 5 shows the master curves of all samples at + 25 °C. The aging-induced stiffening and embrittlement can be observed on all four binders: The complex modulus |G*| is increasing, especially in the lower time–temperature domain, and the phase angle δ is decreasing. Binder 4 seems to be the most aging susceptible one with the highest stiffness increase and phase angle loss, followed by binder 3. Binders 1 and 2 show quite similar evolution with aging at first glance. The following parameters are used for a thorough

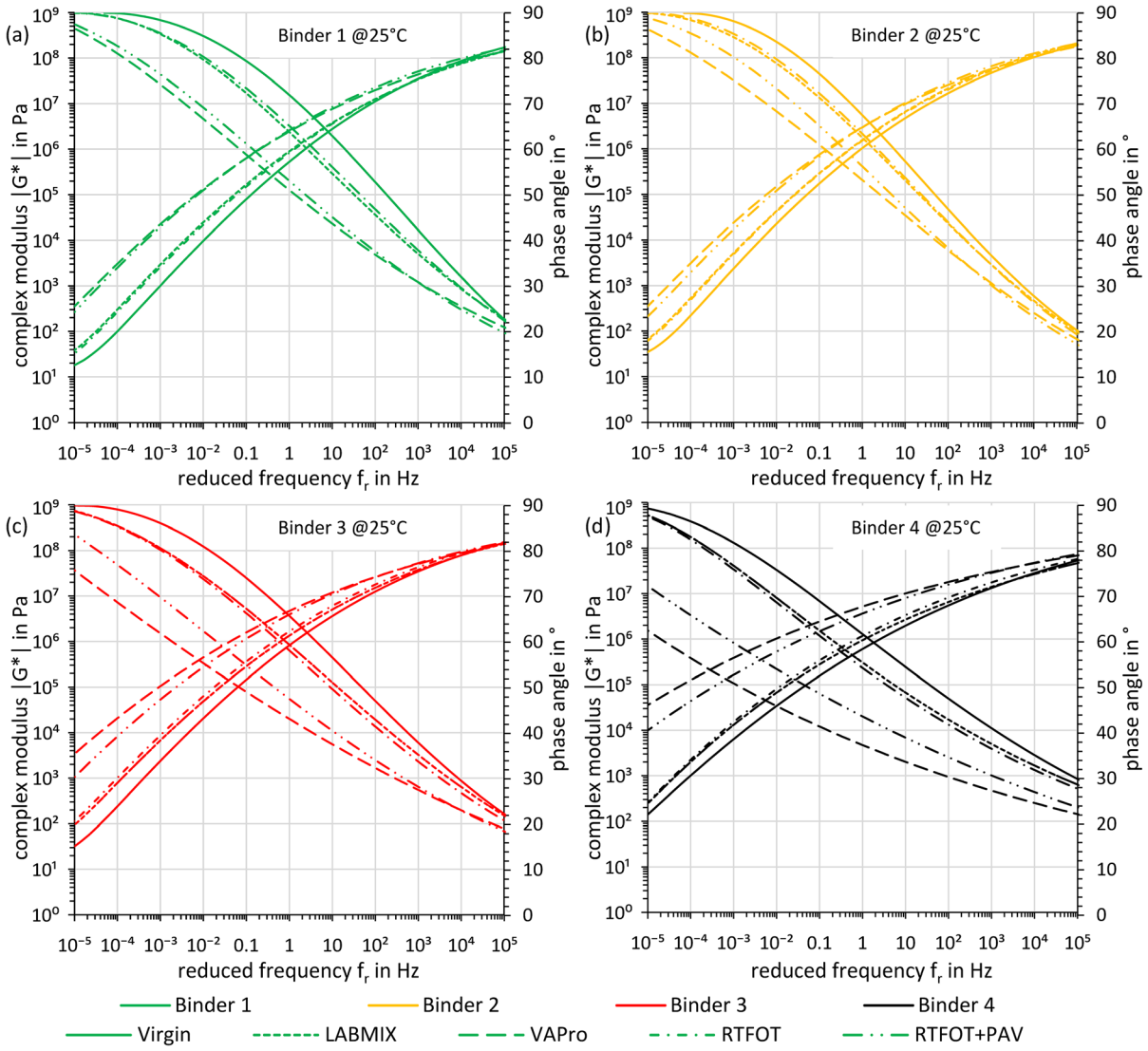

Fig. 5 Mastercurves for shear modulus G* and phase angle δ of all samples at 25 °C; **a** Binder 1, **b** Binder 2, **c** Binder 3, **d** Binder 4

assessment of the aging behavior. The results for each sample are listed in Table 2.

- The rheological parameter R (R-Value)
- Crossover temperature T_c
- Carbonyl index $I_{C=O}$
- G-R parameter

Comparing the crossover modulus G_c given in Table 2, one can observe different development of the respective binders: Binders 1, 2 and 3 have the highest values in the virgin state, ranging from 16 to 27 GPa. Binder 4 is far below with a G_c of 8 GPa, which is roughly in the range of the LTA-aged samples of Binders 1, 2 and 3. This is quite an interesting observation since all four binders have the same grade.

For further mechanical analysis of the investigated binders, attention is put on the R-value and the crossover temperature T_c. Figure 6 shows the link between these two parameters: Considering all samples, a linear correlation with a coefficient of determination of 0.84 can be identified. For each binder, a good linear relationship with aging is observed ($R^2 \geq 0.95$). Every single data point consists of three individual measurements. Standard deviation is between 4 and 5%.

Table 2 Results of the binder analysis

		Virgin	RTFOT	LAB MIX	RTFOT + PAV	VAPro
G_C (GPa)	1	26.77	15.55	13.74	8.63	6.30
	2	20.36	18.01	18.42	13.43	10.34
	3	16.34	11.54	11.86	5.80	3.42
	4	7.77	5.12	4.88	2.86	1.26
R-value	1	1.572	1.808	1.862	2.064	2.201
	2	1.691	1.744	1.735	1.872	1.985
	3	1.787	1.938	1.926	2.236	2.467
	4	2.110	2.290	2.312	2.543	2.901
T_C (°C)	1	5.6	9.1	10.7	18.5	20.1
	2	10.2	12.0	12.3	16.7	18.3
	3	9.4	14.3	12.9	23.7	28.9
	4	11.7	16.8	15.9	28.2	37.1
$I_{C=O}$	1	0.029	0.050	0.051	0.072	0.074
	2	0.032	0.053	0.048	0.066	0.077
	3	0.031	0.048	0.050	0.070	0.083
	4	0.051	0.066	0.066	0.093	0.100
G-R	1	0.11	0.85	1.38	28.33	47.57
	2	0.62	2.,30	2.85	17.50	37.58
	3	0.83	8.25	5.70	109.04	286.84
	4	7.26	36.37	28.48	579.87	1565.05

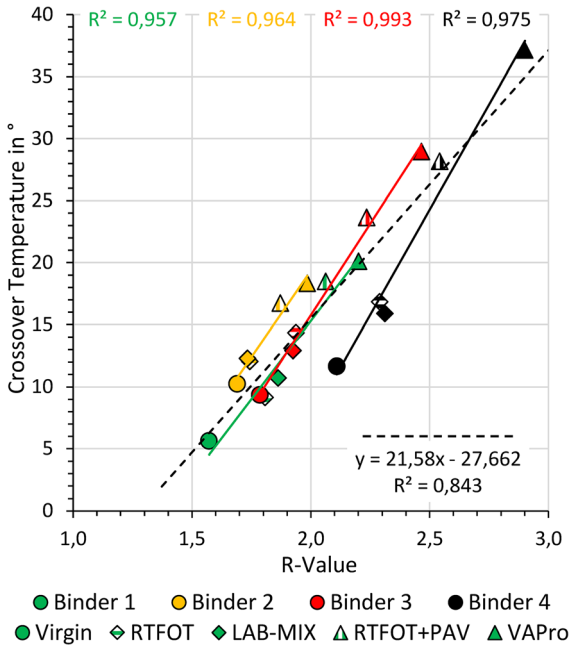

Fig. 6 Link between R-value and crossover temperature T_c

In the virgin state (circles), binder 1 shows the lowest values with an R-value of ~ 1.57 and T_c = 5.6 °C. Binder 2 and 3 behave pretty similar with an R-value of ~ 1.75 and a T_c of ~ 10.0 °C. Binder 4 has the highest values in virgin state with an R-value of 2.1 and a T_c of 11.6.

The STA samples (rhombuses) of binders 1, 2, and 3 range from 1.7 to 1.9 for R-value and from 9 to 14 °C for Tc. This shows that binder 4, in its virgin state, is already at the same level as the STA samples of the other three binders. Although graded the same, binder 4 performs worse than binders 1, 2, and 3 in virgin state and appears already aged.

A similar trend can be observed when looking at the LTA samples (triangles): The STA-sample of binder 4 is already in the range of the LTA samples of binders 1, 2 and 3. The sample of Binder 4 aged with VAPro has the highest values, indicating that it is the most aged or most susceptible to aging. VAPro-aging is also more severe than PAV-aging for all the binders examined.

Similar trends can be seen when looking at the G-R-Parameter in Table 2: VAPro-aging always produces higher values than PAV. The ranking observed in the R-T_c-Diagram is also visible within the G-R-Parameters, identifying binder 4 as most prone to cracking.

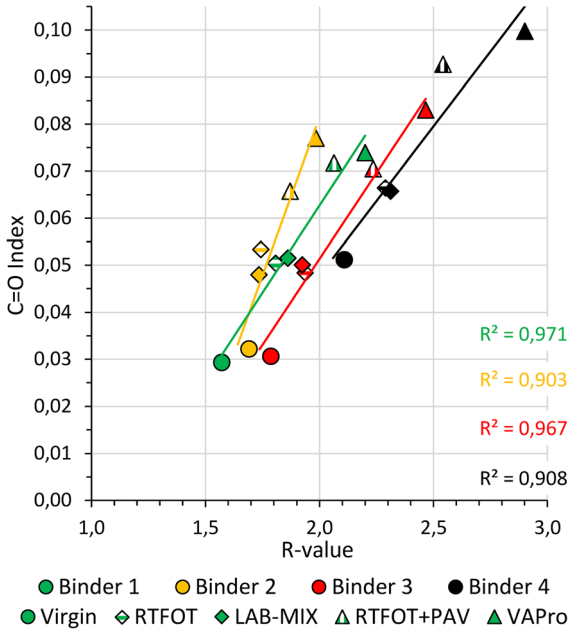

Fig. 7 Correlation of R-value and carbonyl index I_{co}

This shows that VAPro helps in identifying aging susceptible binders. It can point out the differences more pronounced than PAV does. R-Value, crossover temperature T_c and G-R-Parameter are helpful parameters for evaluating the mechanical data. The results show that bitumen of the same grade can have different aging behavior.

To investigate the oxidation state of the bitumen samples, an ATR-FTIR is used. This method is fast and easy to apply. As described in part 2.2.3, only the Carbonyl Index is used for evaluation. Figure 7 shows the correlation between R-Value and the Carbonyl Index I_{co}.

For each bitumen, a good linear correlation is observed. The carbonyl index supports the assumption that bitumen 4 is already aged in its virgin state: It is 0.05 for binder 4, which is on par with the STA samples of binders 1, 2, and 3, with an average of 0.03. You also see the STA of binder 4 is already at the LTA level of binders 1, 2 and 3 and binder 4 is the most oxidized in this diagram. That shows similar behavior as described in Fig. 6. This confirms that binder 4 is more susceptible to aging than the others and is already oxidized in virgin state.

This data set shows that the toolkit of mechanical analysis and chemical analysis, the chemical–mechanical analysis so to speak, is excellent for identifying suitable asphalt binders and sorting out those with poor aging behavior. VAPro-aging points out these differences more clearly than PAV does. Its close-to-field conditions may help evaluate new asphalt mix designs and new additives such as recycling agents or antioxidants more reliably.

4 Summary

This paper shows the application of a recently developed asphalt mix aging method–The Viennese Aging Procedure. VAPro simulates aging processes by perfusing cylindrical specimens with ozone- and nitrogen oxide-enriched air at realistic ambient conditions in terms of temperature and pressure ($T = 60$ °C and $p \leq 1$ bar). Besides the challenge of achieving a homogeneous air void content required for sufficient perfusion, the application of the new aging method was efficiently executed.

The aging behavior of four bitumen of the same grade but different origins is investigated. For reference, the binders are aged in RTFOT and PAV as well. A DSR and an FTIR are used for chemo-mechanical analysis. Three days of VAPro-aging is more severe than RTFOT + PAV–the stiffness increase of the extracted bitumen after VAPro is 1.2 to 2.6 times the RTFOT + PAV level. The dynamic shear modulus |G*| or phase angle δ from DSR and the carbonyl index derived from FTIR show a good correlation and further help evaluating the binders. The sulfoxide index shows differences between VAPro and RTFOT + PAV, possibly due to interactions with the aggregates not present in the PAV. Thus, it is not used for analysis. More research on that phenomenon is needed.

Although being the same penetration grade, the binder source significantly impacts aging susceptibility. This is observable from PAV, but VAPro can distinguish these differences more clearly. Differences seen on the mechanical side can also be overserved by the oxidation state of the binders. FTIR is an excellent tool for evaluating the oxidation of the material [50–53]. This method reveals that one of the virgin binders is already oxidized. Subsequently, this binder shows a higher aging susceptibility. The shown trends in aging susceptibility also correspond to the results of the G-R parameter. In summary, chemo-mechanical analysis offers a valuable tool-set for sorting out poor

performing binders. Further research is in progress, discussing various adaptions of the aging setup, applying the method on binder level for a more fundamental approach, analyzing field aging and VAPro mechanisms and investigating additive behavior with the new approach [54, 55].

Acknowledgements The authors acknowledge TU Wien Bibliothek for financial support through its Open Access Funding Programme. The financial support by the Austrian Federal Ministry for Digital and Economic Affairs, the National Foundation for Research, Technology and Development and the Christian Doppler Research Association is gratefully acknowledged. Furthermore, the authors would also like to express their gratitude to the CD laboratories company partners BMI Group, OMV Downstream and Pittel + Brausewetter for their financial support. The main author greatly appreciates the expert help of all lab technicians and the possibility of using the laboratory infrastructure.

Funding Open access funding provided by TU Wien (TUW).

References

1. EAPA (2020) Asphalt in figures 2019. EAPA, Brussels Belgium
2. Morian N et al (2011) Oxidative aging of asphalt binders in hot-mix asphalt mixtures. Transp Res Rec J Transp Res Board 2207(1):107–116
3. Hagos ET (2008) The effect of aging on binder properties of porous asphalt concrete. University of Technology, Delft, the Netherlands
4. Wei H et al (2019) Aging mechanism and properties of SBS modified bitumen under complex environmental conditions. Materials 12(7):1189
5. Baek C, Underwood BS, Kim YR (2012) Effects of oxidative aging on asphalt mixture properties. Transp Res Rec 2296:77–85
6. Petersen JC (2009) A review of the fundamentals of asphalt oxidation chemical, physicochemical, physical property, and durability relationships. TRB Transp Res Circ E-C140 131:78
7. Hofko B et al (2014) Impact of field ageing on low-temperature performance of binder and hot mix asphalt. In: Kim RY (ed) Asphalt pavements. CRC Press, Boca Raton, pp 381–395
8. Tauste R et al (2018) Understanding the bitumen ageing phenomenon: a review. Constr Build Mater 192:593–609
9. Jing R et al (2019) Laboratory and field aging effect on bitumen chemistry and rheology in porous asphalt mixture. Transp Res Rec J Transp Res Board 2673(3):365–374
10. Bahia HU, Anderson DA (1995) The pressure aging vessel (PAV): a test to simulate rheological changes due to field aging. ASTM International, West Conshohocken, PA, pp 67–88
11. da Costa MS et al (2010) Chemical and thermal characterization of road bitumen ageing. Adv Mater Forum 636–637:273–279
12. Kim YR et al (2017) Long-term aging of asphalt mixtures for performance testing and prediction. The National Academies Press, Washington, DC, p 141
13. Bell CA et al (1994) Selection of laboratory ageing procedures for asphalt aggregate mixtures (SHRP-A-383). Strategic highway research program. National Reserach Counil, Washington, DC
14. Steiner D et al (2016) Towards an optimised lab procedure for long-term oxidative ageing of asphalt mix specimen. Int J Pavement Eng 17(6):471–477
15. Frigio F et al (2016) Aging effects on recycled WMA porous asphalt mixtures. Constr Build Mater 123:712–718
16. Kley D (1997) Tropospheric chemistry and transport. Science 276(5315):1043
17. Atkinson R (1990) Gas-phase tropospheric chemistry of organic compounds: a review. Atmos Environ A Gen Top 24(1):1–41
18. Seinfeld JH, Pandis SN (2016) Atmospheric chemistry and physics: from air pollution to climate change, 3rd edn. Wiley, Hoboken, NJ
19. Hofko B et al (2015) Alternative approach toward the aging of asphalt binder. Transp Res Rec 2505:24–31
20. Hofko B et al (2020) Bitumen ageing–impact of reactive oxygen species. Case Stud Constr Mater 13:e00390
21. Lopes MDM et al (2012) Characterization of aging processes on the asphalt mixture surface. In: 2nd International symposium on, asphalt pavements et environnement, transportation research board of the national academies France
22. Crucho J et al (2018) Tecnico accelerated ageing (TEAGE)–a new laboratory approach for bituminous mixture ageing simulation. Int J Pavement Eng 21:1–13
23. ENS 12697 (2013) Bituminous mixtures–test methods for hot mix asphalt–part 3: bitumen recovery: rotary evaporator. European Committee for Standardization, Brussels
24. EN 13108-1 (2016) Bituminous mixtures - Material specifications - Part 1: Asphalt Concrete. CEN, Brussels
25. EN12591 (2009) Bitumen and bituminous binders. Specifications for paving grade bitumens. CEN, Brussels, Belgium
26. EN 12697-35 (2016) Bituminous mixtures - Test methods for hot mix asphalt - Part 35: Laboratory mixing. CEN, Brussels

27. EN 12697–33 (2007) Bituminous mixtures–test methods for hot mix asphalt–part 33: specimen prepared by roller compactor. CEN, Brussels
28. EN 12697–8 (2019) Bituminous mixtures–test methods–part 8: determination of void characteristics of bituminous specimens. CEN, Brussels
29. EN 12697–6 (2012) Bituminous mixtures–test methods for hot mix asphalt–part 6: determination of bulk density of bituminous specimens. CEN, Brussels
30. EN 12607–1 (2015) Bitumen and bituminous binders–determination of the resistance to hardening under influence of heat and air–part 1: RTFOT method. CEN, Brussels
31. EN 14769 (2012) Bitumen and bituminous binders–accelerated long-term ageing conditioning by a pressure ageing vessel (PAV). CEN, Brussels
32. Maschauer D, Mirwald J, Hofko B (2022) Viennese ageing procedure (VAPro): adaptions and further development to address low-temperature performance of aged asphalt mixtures. Road Mater Pavement Des 23:1–15
33. Steiner D, Hofko B, Blab R (2018) Introducing a nitrogen conditioning to separate oxidative from non-oxidative ageing effects of hot mix asphalt. Road Mater Pavement Des 21(5):1–19
34. EN 14770 (2012) Bitumen and bituminous binders–determination of complex shear modulus and phase angle–dynamic shear rheometer (DSR). European Committee for Standardization, Brussels
35. Kaelble DH (1985) Computer aided design of polymers and composites, vol 7. CRC Press, Boca Raton
36. Rowe GM, Sharrock MJ (2011) Alternate shift factor relationship for describing temperature dependency of viscoelastic behavior of asphalt materials. Transp Res Rec J Transp Res Board 2207(1):125–135
37. Rowe G, Baumgardner G, Sharrock M (2009) Functional forms for master curve analysis of bituminous materials. Advanced testing and characterization of bituminous materials. CRC Press, Boca Raton, pp 97–108
38. Rowe G (2009) Phase angle determination and interrelationships within bituminous materials. Advanced testing and characterization of bituminous materials. CRC Press, Boca Raton, pp 59–68
39. Yusoff NIM et al (2013) Modelling the rheological properties of bituminous binders using mathematical equations. Constr Build Mater 40:174–188
40. Kleizienė R, Panasenkienė M, Vaitkus A (2019) Effect of aging on chemical composition and rheological properties of neat and modified bitumen. Materials 12(24):4066
41. Ganter D et al (2019) Bitumen rheology and the impact of rejuvenators. Constr Build Mater 222:414–423
42. Planche J-P et al (2019) Linking binder characteristics with performance: the recipe to cope with changes in bitumen binder quality. In: 26th World road congress world road association (PIARC)
43. Garcia Cucalon L et al (2019) The crossover temperature: significance and application towards engineering balanced recycled binder blends. Road Mater Pavement Des 20(6):1391–1412
44. Christensen DW, Anderson DA (1992) Interpretation of dynamic mechanical test data for paving grade asphalt cements (with discussion). J Assoc Asph Paving Technol 61:67–116
45. Reinke G et al (2016) Impact of re-refined engine oil bottoms on binder properties and mix performance on two pavements in Minnesota. In: Proceedings of the E&E congress
46. Margaritis A et al (2020) Identification of ageing state clusters of reclaimed asphalt binders using principal component analysis (PCA) and hierarchical cluster analysis (HCA) based on chemo-rheological parameters. Constr Build Mater 244:118276
47. Glover CJ et al (2005) Development of a new method for assessing asphalt binder durability with field validation. Texas Dept Transp 1872:1–334
48. Rowe G, King G, Anderson M (2014) The influence of binder rheology on the cracking of asphalt mixes in airport and highway projects. J Test Eval 42(5):1063–1072
49. Sreeram A et al (2021) Accelerated aging of loose asphalt mixtures using ozone and other reactive oxygen species. Constr Build Mater 307:124975
50. Hofko B et al (2017) Repeatability and sensitivity of FTIR ATR spectral analysis methods for bituminous binders. Mater Struct 50(3):1–15
51. Hofko B et al (2018) FTIR spectral analysis of bituminous binders: reproducibility and impact of ageing temperature. Mater Struct 51(2):1–16
52. Weigel S, Stephan D (2017) The prediction of bitumen properties based on FTIR and multivariate analysis methods. Fuel 208:655–661
53. Lamontagne J et al (2001) Comparison by Fourier transform infrared (FTIR) spectroscopy of different ageing techniques: application to road bitumens. Fuel 80(4):483–488
54. Mirwald J et al (2020) Impact of reactive oxygen species on bitumen aging–the Viennese binder aging method. Constr Build Mater 257:119495
55. Werkovits S et al (2023) The impact of field ageing on molecular structure and chemistry of bitumen. Fuel 343:127904